IOPscience iopscience.iop.org

Home Search Collections Journals About Contact us My IOPscience

Deposition from a drop: morphologies of unspecifically bound DNA

This article has been downloaded from IOPscience. Please scroll down to see the full text article.

2005 J. Phys.: Condens. Matter 17 S703

(http://iopscience.iop.org/0953-8984/17/9/025)

View the table of contents for this issue, or go to the journal homepage for more

Download details:
IP Address: 129.252.86.83
The article was downloaded on 27/05/2010 at 20:25

Please note that terms and conditions apply.

INSTITUTE OF PHYSICS PUBLISHING JOURNAL OF PHYSICS: CONDENSED MATTER

J. Phys.: Condens. Matter **17** (2005) S703–S716 doi:10.1088/0953-8984/17/9/025

Deposition from a drop: morphologies of unspecifically bound DNA

T Heim[1], S Preuss[2], B Gerstmayer[2], A Bosio[2] and R Blossey[1]

[1] 1 Interdisciplinary Research Institute, c/o IEMN Avenue Poincaré BP 69, F-59652 Villeneuve d'Ascq, France
[2] Memorec Biotec GmbH, Stöckheimer Weg 1, 50829 Köln, Germany

Received 24 November 2004
Published 18 February 2005
Online at stacks.iop.org/JPhysCM/17/S703

Abstract

We have studied the morphologies of unspecifically bound DNA on solid substrates that arise when it is deposited from a liquid drop. Depending on the mode of removal of the liquid from the surface, and on the properties of the solvent and substrate, the observed single-molecule morphologies range from elongated to condensed conformations. Further, we have examined the amount of unspecifically bound DNA on microarrays deposited from drying droplets, for which we have employed test systems based on gene fragments of *E. coli* and oligonucleotides.

(Some figures in this article are in colour only in the electronic version)

1. Introduction

Interfacial instabilities occur ubiquitously in liquids at surfaces. A prominent example is the dewetting of ultrathin films: here, the two basic instability mechanisms are either (homogeneous or heterogeneous) nucleation or spinodal dewetting [1]. Meanwhile, in a combined effort of experimentalists and theorists, a very good quantitative understanding of these processes has been achieved [2–5]. Thin film instabilities can also be triggered by defects, such as vortices in undercooled wetting films of helium on alkali metals [6–8] or by the application of thermal gradients to confined polymer films [9–11]. For the helium films, the situation is slightly complicated due to the pronounced substrate disorder effects [12, 13] which, however, are irrelevant for the strongly asymmetric thermal hysteresis that is common to all wetting systems [14, 15, 1].

Another particular case of wetting-related instabilities, e.g., arises in solid-like semiconductor systems, where, upon a surface layering process, quantum dots may undergo a morphological change into quantum rings [16, 17]. An even more common ring-forming process has been discussed by Deegan *et al* who elucidated the origin of the ubiquitous 'coffee-stain' effect, i.e., the formation of the ring-shaped remains of dried-out coffee droplets [18–20]. Subsequently, this problem has raised widespread interest in the research community—not

 © 2005 IOP Publishing Ltd Printed in the UK

as the daily nuisance that it causes, but because of its technological relevance. Droplet-based deposition of materials is a very common process ranging from inkjet printers to DNA microarrays [21]. In particular in the latter case, the coffee-stain effect—known as the 'doughnut effect' in the biotechnology community—is a well-known problem, circumvented often by elaborate image analysis techniques rather than a change in the physics and chemistry of the deposition process. The formation of ring-shaped deposits originating from evaporation of the solvent had also previously been observed in thin films of organic solutions of porphyrin molecules, for which a tentative morphology diagram was put forward [22].

In this paper, we return to the relationship of droplets on surfaces and the deposits that arise from them. Beyond our previous studies on this issue [21, 22], we consider the overall motion of the liquid droplet, and we focus on the deposition of single molecules rather than a dispersed solute. To be specific, we address one particular aspect of droplet-based deposition: how does the way the liquid is removed from the surface affect the deposition of DNA, and what are the morphologies of DNA at the surface? In all cases, DNA is unspecifically bound to the surface. Unspecific binding here means that the binding state is controlled by intermolecular forces (such as electrostatic forces), and not by molecular interactions leading to the formation of covalent bonds. The binding of strands of DNA, by contrast, is generally referred to as hybridization, be it that of complementary strands or that of strands with mismatches. We address the question from the single-molecule perspective in order to elucidate the influence of several experimental factors on the possible surface morphologies of DNA.

We first give a brief introduction to the physics of evaporating droplets and the deposition mechanisms for the solute that the solvent contains. We then describe the single-molecule experiments that we have performed. Finally, we discuss experiments on DNA deposition on cDNA microarrays, performed in order to understand the effects of unspecifically bound DNA in such systems. We close with a discussion and an outlook on further directions of study.

2. Depositing DNA from drops: a brief introduction

The deposition of DNA (or other molecules, for that matter) by liquid droplets is affected by dynamic processes in the bulk of the liquid and at its interfaces. The classical example of the coffee stain in dried out droplets illustrates this. The process which generates these structures is driven by evaporation of the solvent from the bulk of the drop. Thus, the droplet volume shrinks and, if the contact line of the drop remains rigidly pinned, the droplet shape undergoes a change of its contact angle during the evaporation process. Evaporation is most effective at the rim of drop, where the probability that an evaporated solvent molecule recondenses to the drop is less than that near the centre of the drop. The essential physical quantity then is the evaporation current in the vicinity of the drop edge on the substrate $r = R$ which behaves as [18]

$$J_s \propto (R - r)^{-\lambda} \tag{1}$$

where the exponent depends on contact angle θ via

$$\lambda = \frac{\pi - 2\theta}{2\pi - 2\theta}. \tag{2}$$

This result is obtained by solving the Laplace equation for the vapour mass per unit volume u, $\nabla^2 u = 0$, to which the diffusion equation for u reduces when stationary conditions are reached rapidly. The problem then is analogous to solving Poisson's equation for a lens-shaped capacitor. In this analogue example, u is equivalent to the electrostatic potential, and the evaporation current J_s corresponds to the electric field, E.

Under these conditions, the mechanism that drives the dissolved material to the droplet edge is convection. It is governed by the equation for the local solute concentration, $c(r, t)$ [21],

$$h(r, t)(\partial_t c(r, t) + v(r, t)\partial_r c(r, t)) = \frac{c(r, t)}{\varrho} J_s \sqrt{g} \tag{3}$$

where h is the height of the drop, ϱ is the liquid density, $\sqrt{g} = \sqrt{1 + (\nabla h)^2}$ is the surface element of the drop, and $v(r, t)$ is the interfacial velocity. Note that h is the local drop height, which is governed by its own dynamical equation (usually written down in a lubrication approximation to the Navier–Stokes equations) [20].

The dominance of convection over diffusive behaviour explains why, usually, material assembles at the droplet edge and accumulates into ring-shaped deposits of increasing mass $m_R \sim t^{2/(1+\lambda)}$ at the early stages of ring formation. At late times, the ring mass 'diverges', as $dm_R/dt \sim (t_f - t)^{-0.25}$ [20].

This whole description, however, rests on the *assumption* that diffusion of the solute in the drop does not arise. Experiments have generally confirmed this [19]. Two of us (AB and RB) have recently presented evidence for a convective deposition mechanism obtained from an analysis of cDNA deposits [21]. Our results showed that the deposit shapes that we observed on the cDNA microarrays contain significant deviations from the toroidally shaped ring deposit whose origin we could trace back to the spotting process. The fast convection process maintains a memory of the initial solute distribution in the drop which is reflected in the shape of the ring deposits. This memory effect would have been washed out if the given diffusive processes had been sufficiently strong.

The effect of interfaces on the deposition of molecules at a substrate is most clearly seen in the molecular combing technique, pioneered by Bensimon and co-workers [23–25]. Here, a substrate is pulled out of DNA-containing solution; the set-up is similar to that of a Langmuir trough. The liquid meniscus recedes along the pulled-out surface and the DNA molecules are oriented perpendicular to this interface. The results of this manipulation are then molecular distributions of parallel DNA at the substrate.

Such elongation or stretching of DNA on a substrate is also possible at the boundary of a liquid drop. As recently pointed out by Abramchuk *et al*, single molecules in the convection flow at the droplet rim can be fully elongated [26, 27], while in the vicinity of the droplet centre, the molecules remain in their coil state. These states were observed under addition of polyethylene glycol (PEG), which prevents the occurrence of ring-stained deposits at the droplet rim. Interestingly, in these experiments, the elongated DNA molecules essentially have their natural end-to-end distances, while typically combed DNA is considerably overstretched (1.2–1.5 times the natural contour length). Apparently, the degree of stretching depends on the details of the surface preparation.

These results indicate that the mechanisms exerted on DNA molecules in liquid droplets are worth further study. This problem is not only of fundamental interest, but may also have interesting implications for the design of cDNA microarrays. It is becoming increasingly clear that cDNA microarrays, despite their basic simplicity, are a highly complex research instrument with a number of as yet unresolved features [28]. We, and others, expect a better understanding of the physical mechanisms of these systems to lead to a much improved design of bioanalytical devices.

3. Depositing DNA from drops: experiments

We now turn to the description of our experiments in which DNA was deposited from a drop placed on top of surface-treated silicon wafers. (These surfaces were selected, as silicon

oxide surfaces are the most common substrates for technical applications.) The samples are prepared as follows. Silicon wafers are cleaned in piranha solution (H_2SO_4:H_2O_2 in a 2:1 ratio) which leads to highly hydrophilic surfaces rich in OH termini. In order to obtain a hydrophobic or charged surface we chemically treat the surface with silanizing agents and polymers: octadecyltrichlorosilane (OTS) and polystyrene (PS) for a hydrophobic surface, and 3-aminopropyltrimethoxysilane (APTMS) for a positively charged surface.

In the case of the OTS surface, the freshly cleaned substrate was dipped in the silanization solution (the molecules are dispersed in hexadecane solvent, 10^{-3} M) for 2 h in a nitrogen atmosphere. This silanization procedure is known to form a 2.5 nm thick self-assembled monolayer (SAM) of OTS. The molecules form 2D crystalline phases exposing their methyl end-group (–CH_3). The contact angles of $\theta_{\text{water}} = 108°$–$110°$ and $\theta_{\text{hd}} = 43°$ are a signature of well-packed CH_3-terminated surfaces [30].

Polystyrene (diluted in toluene) is deposited by spin-coating. The thickness of the deposit layer is in the range of 100–200 nm, depending on the viscosity of the polymer solution and the rotation speed. The contact angle for water then is $\theta_{\text{water}} = 90°$ [31].

Finally, the deposition of APTMS is performed in the gas phase. The freshly cleaned substrate is deposited in a desiccator flushed with nitrogen. APTMS is added in a beaker next to the surface and left there for some hours. The molecules evaporate in the desiccator and coat the surface by hitting it randomly. After exposure, the surfaces can be stored without additional precautions. The thickness of the coating layer is a function of the exposure time; 6 h of exposure lead to a 2 nm thick layer. This procedure leads to a flat surface with a water contact angle of $\theta_{\text{water}} = 70°$–$80°$.

All our single-molecule deposition experiments were performed using λ-phage DNA (16 μm long, 50 000 bp) purchased from Roche-Biomedicals. The molecules were dispersed in buffer (Tris/EDTA (10 mM/1 mM) or Mes/EDTA (10 mM/1 mM)) at a pH varying from 5.0 to 9.0. The deposited DNA is characterized by AFM and fluorescence microscopy. We have always aimed at reaching a correspondence between the results obtained by both methods. For the latter, the DNA is intercalated with YOYO-1 dyes [29] ($\approx$1 dye about every 20 bp) by mixing solutions of the two molecules for a few hours. In all cases, we have determined the stretching state of DNA and its amount can be detected by measuring the height of the deposits with AFM. An overstretched DNA molecule is flatter than its crystallographic diameter, and the presence of several DNA molecules leads to height values larger than the crystallographic value. The length of the DNA can be independently measured by means of fluorescence and again compared to the crystallographic length of the molecule.

We now turn to the description of our droplet-based DNA deposition methods, which are illustrated in figure 1. For all these methods, the samples are covered during the time of incubation to reduce and control the effect of evaporation.

Method (A). A drop of the buffer solution containing DNA (at 250–500 ng μl^{-1}, i.e., 10–20 pM) was put on the surface, left for a few minutes for incubation and then removed by tilting the substrate. In this method, both volume-and interface-controlled effects on deposition can be observed depending on whether the air–water interface contacts the substrate or not. The DNA spreads during the incubation time at the air–water interface. If the removal of the drop is very fast the air–water interface can be prevented from touching the sample surface [25]. In this case, DNA deposition is homogeneous all over the surface in contact with the solution during the incubation time; see figure 1(a). As in molecular combing, the molecules are overstretched on a hydrophobic surface, in contrast to the charged surfaces case; see figure 1(b).

If, by contrast, we allow the air–water interface to contact the substrate, DNA can be transferred from the air–water interface to the solid substrate. The critical step then is the removal of the solution using microdiffusion techniques [34–38]. We have shown that it is

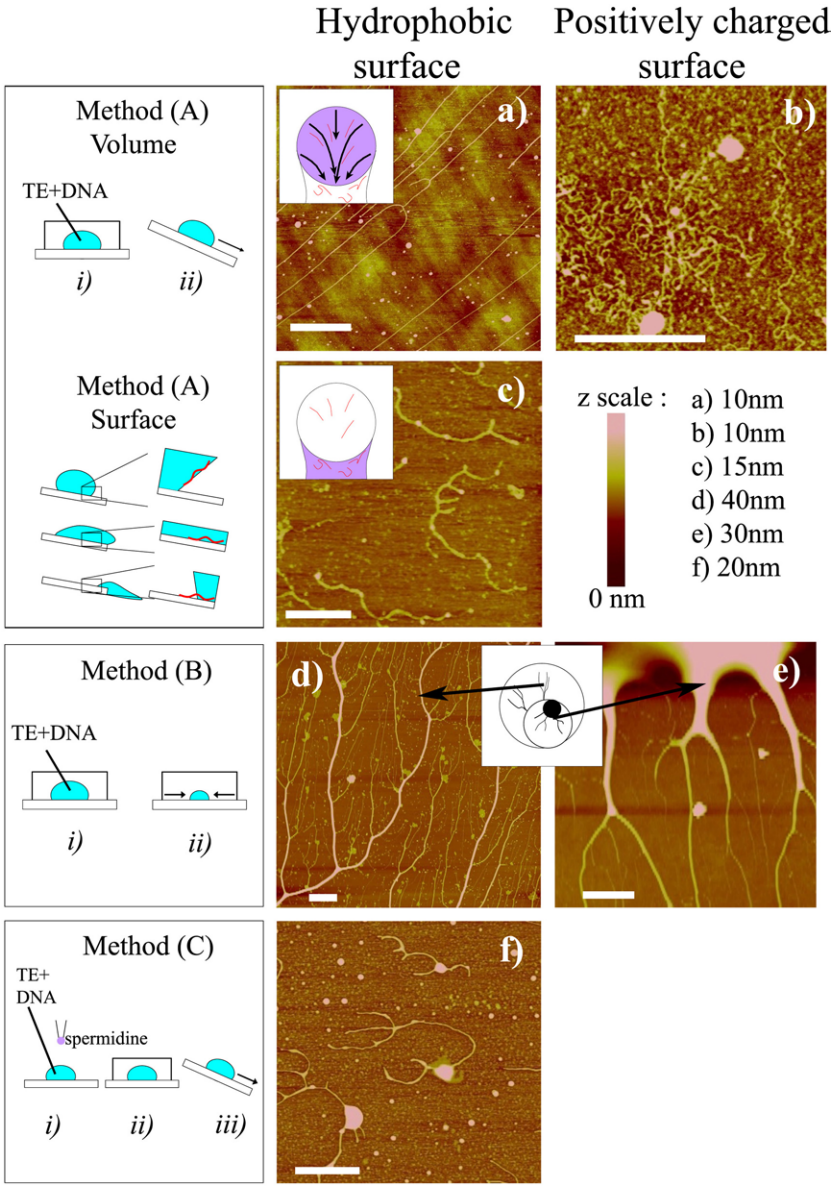

Figure 1. Three different methods of droplet-based DNA deposition on hydrophobic and positively charged surfaces. All pictures were taken by AFM; the colour code refers to height values and is shown in the graph. λ-DNA is dispersed in Tris(10 mM)/EDTA(1 mM) buffer (pH = 6–7) to a final concentration of 10 pM. DNA deposition occurs in two steps: grafting of the molecule on the surface, then removal of the solution. The shape of the DNA depends on these two steps. Straight DNA molecules are obtained on hydrophobic surfaces by method (A) (shown in (a)). The orientations of the molecules at the position of the drop are indicated by arrows in the inset. With the same method, DNA has a coil conformation on positively charged surfaces in (b). In the second case with this method, DNA molecules are deposited by the transfer from DNA spread at the air–water interface. The molecules are deposited at the edge of the sample as indicated by inset (c). With method (B), DNA forms orientated ropes independently of the wetting properties of the surface (shown in (d) and (e)). Method (C) is performed on a hydrophobic surface. The adjunction of spermidine (a condensing agent) results in the condensation of molecule already grafted on the surface in isolated DNA ropes; see (f). The grafting point of DNA prevents the complete folding of the molecules. Scale bars for all images are 1 μm.

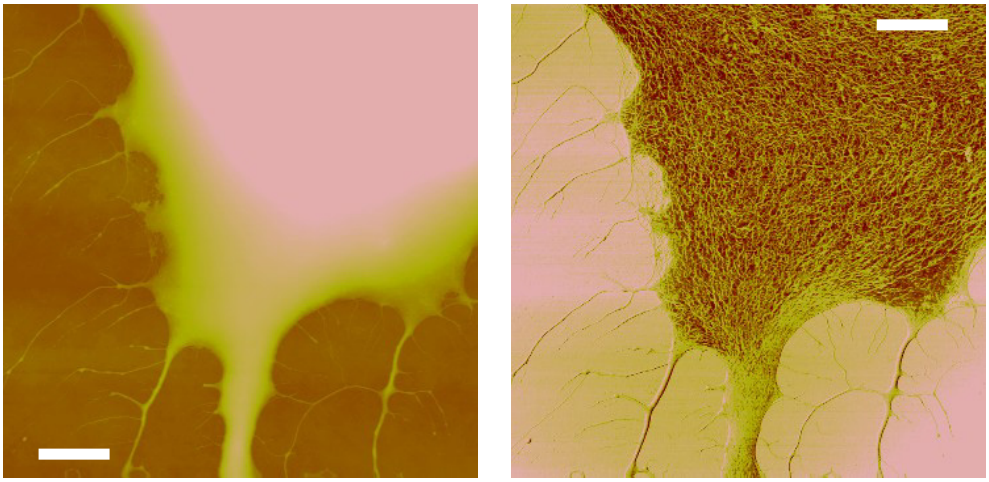

Figure 2. A topographic and phase image in atomic force microscopy (intermittent contact mode) of DNA prepared by method (B) in the vicinity of the DNA gel. DNA molecules in the gel look like a spaghetti plate visible in the phase image. DNA molecules orient themselves when forming ropes connected to the gel. The scale bar is 1 μm.

possible to deposit DNA by this technique on an OTS surface. The transferred DNA is observed between the initial position of the drop and the edge of the sample as shown in figure 1(c). The air–water interface touches the OTS surface only for a brief instant during the liquid removal, enough for the deposition of DNA to occur. The molecules are not overstretched and never cross on the surface. Here, Brownian motion in two dimensions gives a coil conformation of DNA with an end-to-end distance larger than in solution [39], leading to an almost fully elongated, but not overstretched conformation of DNA; see figure 1(c).

Method (B). In method (B) the drop is left evaporating at the surface. This corresponds to an increased incubation time ($\sim$5 h), and also to an increase of buffer and DNA solution concentrations within the drop during the evaporation process. This procedure results in the formation of straight DNA ropes (i.e., multiple DNA molecules wound around each other) of sizes ranging from a few DNA molecules to few thousand (assuming a DNA cross-section of 3 nm^2), organized in tree-shaped structures, as seen from figures 1(d) and (e). This result is found independently of the wetting properties of the surface.

The DNA deposition is not uniform on the substrate, as illustrated in the inset of figure 1(d). The drop is partially pinned at the contact line during the evaporation process, and moves about on the surface. The drying of the drop leaves a large amount of salt and DNA in circular shapes in a central region of the droplet at the end of the drying process. The DNA in these structures is very concentrated and forms a gel-like phase. The AFM phase image of figure 2 shows the DNA molecules embedded in a gel structure—similar to spaghetti on a plate. DNA ropes remain connected to the gel, which is sufficiently stiff to sustain the AFM measurement [32].

Method (C). In method (C), first a 40 μl drop of DNA in buffer solution is deposited on a hydrophobic surface as in method (A). After a few minutes, a 1 μl drop of spermidine (1 M, pH $\sim$ 7) is added which enhances the interaction between the DNA molecules [33]. After 30 min of incubation the drop is removed by tilting the sample. The morphology of the DNA after deposition is shown in figure 1(f). As expected from the use of spermidine as a condensation agent we do not observe straight DNA ropes oriented by the receding meniscus

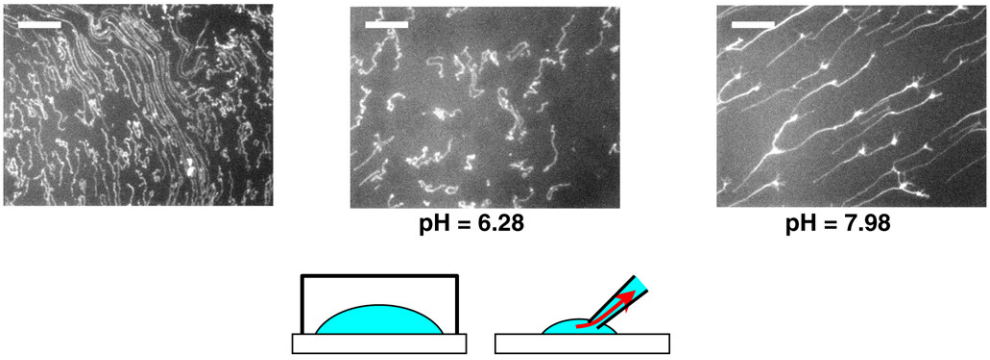

Figure 3. DNA deposition by deposition from the air–water interface on hydrophilic substrates at three different pH values. The DNA solution is composed of 10 pM ADN in MES(10 mM)/EDTA(1 mM) buffer. Removal of the drop is performed by aspiration with a micropipette. The shape of the DNA varies from an elongated self-avoiding molecule to DNA ropes orientated by the moving meniscus as the pH increases. The scale bar is 10 μm.

as in the overstretched case of method (A), but rather separated ropes of 5–20 nm in diameter showing no preferential orientation. We do not observe other DNA morphologies such as molecular 'doughnuts', 'croissants' and rod shapes on the surface. The absence of these structures comes from the low grafting efficiency of the condensed DNA on the surface [23–25]. In practice, the condensed DNA ropes in method (C) arise from the action of spermidine on DNA molecules that are already grafted to the surface prior to the addition of the spermidine droplet. This is confirmed by the observation that no DNA deposition could be obtained when droplets of pre-mixed DNA and spermidine solutions are used for deposition.

We also tried a further variation of the methods to transfer DNA, which is shown in figure 3. In this case the DNA solution is deposited on a hydrophilic substrate ($\theta_{\text{water}} = 47°$). With method (A), DNA deposition on this substrate does not occur. The surface is obtained by the exposure of a clean substrate to OTS vapour and by pipetting the solution with a micropipette. The air–water interface is put into contact with the substrate. The effect of the meniscus is not negligible at higher pH (around 7–9) and it results in an alignment of DNA in the form of ropes as shown in figure 2.

Quite generally, the removal of the drop by aspiration with a micropipette is disadvantageous. Material at the air–water interface (salt, DNA) then cannot come into contact with the substrate, and the DNA deposition is not homogeneous at the surface. In particular, the deposition strongly depends on the salt content. The formation of hydrophilic (i.e., salt-rich) regions on the hydrophobic substrate is then a typical signature. On the sample dried by this procedure we observe the formation of salt crusts of about 6–7 nm height (see figure 4).

We now integrate our findings by methods (A)–(C) into a common picture via a discussion of the properties of the DNA assemblies at the different surfaces. In the case of method (A), we studied the morphology of DNA (length, height, density, ...) on the surface. On a hydrophobic surface this method leads to overstretched ropes of a few (<5, typically) DNA molecules exhibiting an orientation perpendicular to the moving liquid–air meniscus, similar to the findings of [25]. This technique gives a reproducible DNA stretching independently of the pH value. In our experiments, DNA molecules exhibit at most a few grafting points with the surface and always preferentially bind with their ends [40]. The force exerted by the meniscus on DNA is responsible for this elongated state. The overstretching of DNA has been checked by fluorescence microscopy (not shown). Its value is around 150–170% of the crystallographic length of λ-DNA (16.5 m). On the aminated surface, DNA always has a coil conformation, as

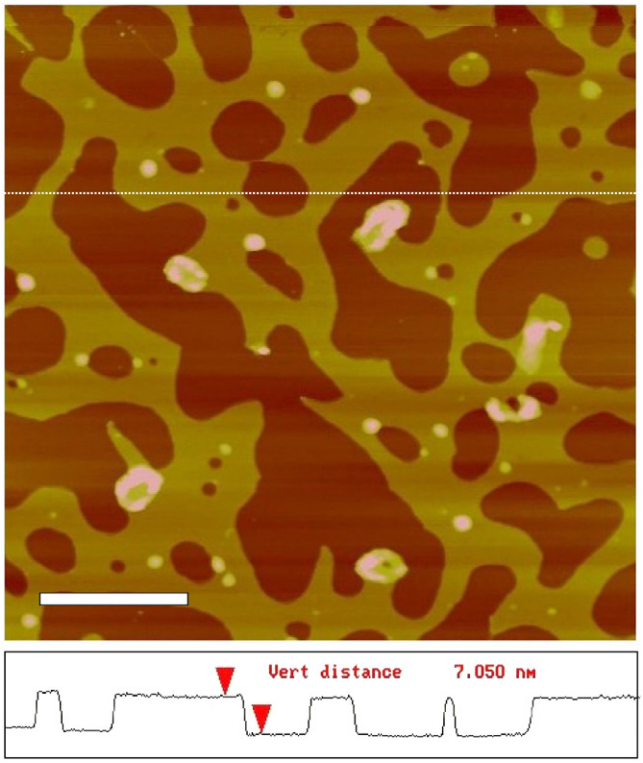

Figure 4. The salt crust left on an OTS surface during the drying procedure. Holes in the salt crust as seen by scanning with an AFM tip. 'Croissant'-shaped DNA molecules are embedded in the salt crust and seen as bright spots. The composition of the DNA–buffer solution is: 10 pM ADN, Tris(10 mM)/EDTA(1 mM), pH = 6.5, 200 mM spermidine. The scale bar is 1 μm. The height variation is indicated by the AFM scan.

shown in figure 1(b). Aminated surfaces are positively charged as the pKa $\approx$ 9 of the surface. DNA thus adsorbs strongly on this surface. The shape of the DNA results from a projection of the DNA floating in bulk onto the surface. The DNA shape is thus not altered by the drying procedure. In flow, DNA can be elongated as stretched by the movement of the solution in the vicinity of the surface. We measure a length of around 16 μm close to the expected value for λ-DNA.

Salt composition and the pH of the buffer solution affect the DNA density only on the hydrophobic surface. DNA in a salt buffer at low concentrations (10 μM Tris) does not bind to the hydrophobic surface. The presence of salt is required to screen the electrostatic repulsion between the DNA and its image charge caused by the insulating surface (OTS or PS). Hence the density of the DNA molecule on the surface is related to the amount of cations in the solution. Tris buffer solution (which is neutral above pH = 8.1 and positively charged below pH = 8.1) contains a higher concentration of cations than MES buffer (which is negatively charged above pH = 6.1 and neutral below pH = 6). Thus, the amount of cations increases as the pH decreases for both buffers. This observation partially explains the variation of DNA density versus pH and buffer, as shown in figure 5(a).

Another explanation of this variation is related to the mechanism of grafting. It consists in the local opening of the double-helical structure of DNA favoured at low pH, exposing base pairs to the hydrophobic surface. This mechanism enhances the hydrophobic interaction

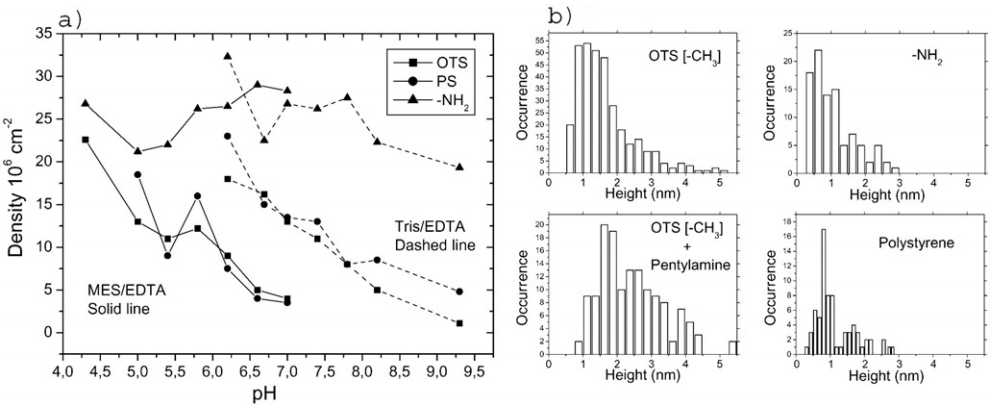

Figure 5. The height and density of DNA molecules. The height of the DNA is measured on a hydrophobic surface (OTS and PS) for DNA molecules deposited by method (A) and on an aminated surface for ones deposited by method (B). The height of the molecule increases on addition of pentylamine on the hydrophobic OTS surface. The density of the molecules decreases as the pH increases for the hydrophobic surface in the case of method (A), and is constant for the amine surface. Tris(10 mM)/EDTA(1 mM) is a more efficient buffer than MES(10 mM)/EDTA(1 mM) for DNA deposition at a given pH.

between the DNA and the surface. In the case of an aminated surface the interaction between DNA and the surface is dominated by electrostatic interactions between the negatively charged DNA and the positively charged surface. The density of DNA molecules on this surface increases as $\sqrt{t}$ during deposition. The exponent of 0.5 is expected in the case of a mechanism of diffusion and trapping on the surface. For hydrophobic surfaces (OTS and PS), the exponent is around 0.2–0.3 [31, 41]. This means that DNA molecules can approach the hydrophobic surface without being trapped.

Finally, we address the height of the DNA molecules on the surface. On an aminated surface, the maximum observed height of DNA is around 0.5 nm, to be compared with an expected (crystallographic) value of 2.4 nm [42]. The considerably flattened conformation of DNA is certainly due to a strong interaction between the DNA and the surface, resulting in a deformation of the double-helical structure of the molecule. In the case of a hydrophobic surface we measure 0.8 and 1 nm for PS and OTS, respectively. In the case of the PS surface the histogram exhibits two peaks at $H_0 \approx 0.8$ and $2H_0 \approx 1.75$ nm, consistent with the height of one and two DNA molecules. On the hydrophobic surface, the flattened conformation of DNA can be explained by the overstretching of the molecule. The deposition of method (A) in the presence of a pentylamine diminishes the contact angle of the drop, and hence the stretching force of the meniscus [25] results in non-overstretched DNA on the surface; see figure 6 [43]. In this case, the height of the molecules is 2.8–2.9 nm (see figure 5(b)).

4. Depositing DNA from drops: microarrays

In this section, we describe experiments on the role of unspecific binding of DNA on cDNA microarrays. Here, we do not look for the morphology of the molecules; certainly, a wide variety of different morphologies will arise. Instead, we focus on the presence or absence of unspecific binding, since it is a nuisance for these technological systems. The substrate surfaces (glass slides) of cDNA microarrays are usually prepared to allow a covalent attachment of the DNA with one of its extremities. Thus, typically the end of one chain may contain, e.g., a linker

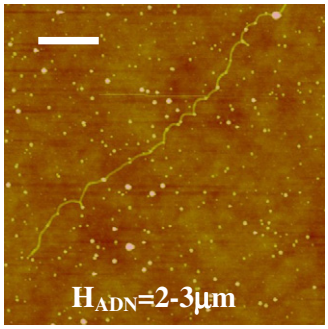

Setpoint A/A_0	H_{ADN} (nm)	
0.8	1.6 - 1.7	
0.85	1.5 - 1.9	
0.92	1.6 - 2.3	
0.95	2.4 - 2.6	Light tapping

Figure 6. DNA on an OTS surface deposited by method (A) in the presence of pentylamine. The molecules are not overstretched as observed in the case of method (A). The height of this molecule is 2–3 nm. The scale bar is 1 μm. The height of the DNA molecules deposited by method (A) in the presence of pentylamine depends on the imaging conditions as shown in the accompanying table (molecule not shown). A and A_0 are, respectively, the amplitude and the free amplitude (without the tip–surface interaction) of the AFM tip. From a low set-point to light tapping conditions (i.e. force on DNA applied by the AFM tip decreasing), the height of DNA increases. DNA in that case behaves like a soft material. The histogram of DNA heights deposited in the presence of pentylamine is shown in figure 5.

molecule carrying an amino group. Aside from the specific, covalent binding to the substrate, unspecific binding occurs, which is unwanted from a technological point of view.

In order to assess the role of unspecific binding in these systems, we have performed a series of experiments employing the standard preparation conditions for commercial microarrays [44]. Our test systems were based on fragments of different *E. coli* genes (in the range of 200–500 bp) and 15 bp long oligonucleotides. The *E. coli* fragments were amplified (copied) in a vector–PCR reaction in the presence of fluorescence dyes (Cy3-dCTP) which are commonly used in the commercial microarrays. The coding strand was selected to carry the amino group for linking to the silanized substrate glass surface.

The oligonucleotides were prepared in two fashions. First, two variants were made, once with and once without the amino linker molecule. Secondly, the fluorescent labelling of the oligonucleotides was either prepared using the Cy3 system, while in a second system biotinylated oligonucleotides were subsequently stained with streptavidinylated Cy3. The cDNA was spotted onto silanized glass substrates, essentially by method (B), using an automated spotting system (akin to an inkjet printer system). The droplets are left to dry out on the substrate; usually, the contact lines of the drops are rigidly pinned due to the roughness of the glass substrates.

The double-stranded *E. coli* fragments on the substrates are then heated (95 °C, 2 min) in order to denature (dissociate) the double-standed DNA. After washing of the slides, the fluorescence intensity was measured. A 50% fluorescence signal of the originally spotted double-stranded DNA is then to be expected if all DNA had been originally attached to the substrate in a covalent fashion. (Over a wide range of intensities, the relationship between fluorescence intensity and amount of material present is linear, and only deviates for large

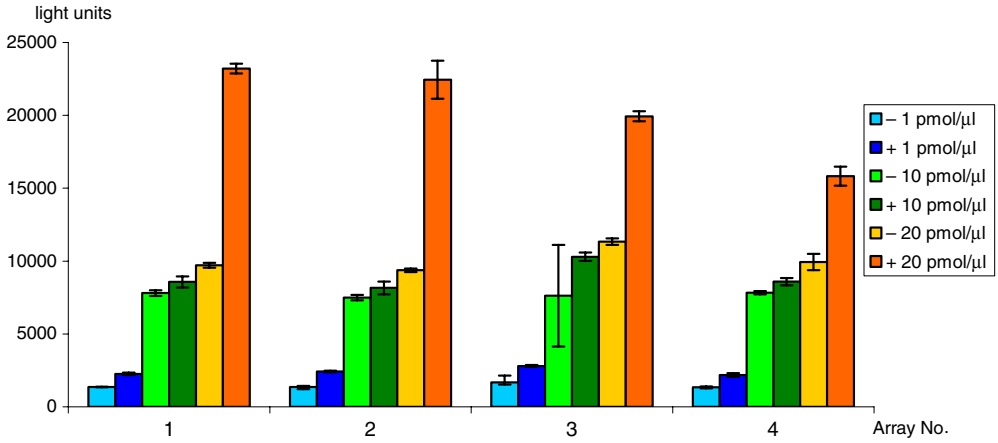

Figure 7. Net light intensities of Cy3-marked oligonucleotides after denaturation, based on four different microarrays. Scanner: arrayWoRx (Cy3 585/595), 0.1 s). Key: − oligonucleotide carries no amino linker; +: oligonucleotide with amino linker.

amounts of material due to quenching effects.) Largely independently of fragment length, however, a 60–70% signal is found. Thus, additional unspecific binding of fluorescently labelled DNA must persist at the surface which is not removed by the washing steps.

In a control experiment with the Cy3-labelled oligonucleotides, we have measured fluorescence intensities after denaturation, varying the amount of spotted oligonucleotides from 1 to 20 pM μl^{-1} in the drop. We find that for low concentrations, almost no difference in signal occurs when comparing the systems with and without amino linkers; see figure 7. Only at the highest concentrations do we find a significant difference (a factor between 2 and 2.5) between the covalently bound and non-covalently bound oligonucleotides. Evidently, at the highest concentrations, the process of covalent attachment begins to dominate over the non-specific binding mechanism.

The origin of this non-specific binding can be traced back to the fluorescent labels. Hybridization of the spotted, labelled *E. coli* fragments with Cy3-labelled *in vitro* transcripts yields a roughly fivefold higher fluorescence signal from the molecules with amino linker when compared to those without. In addition, we find a strong dependence of the signal from the unspecifically bound DNA on gene length: a factor of two change in gene length increases the fluorescence signal by a factor of 8–10 (figure 8). We thus are led to conclude that a significant contribution to the non-specific binding of cDNA to the surface is due to the interaction between the fluorescent labels and the substrate.

In order to check this result further, we finally compared it with the oligonucleotides with the biotin–streptavidin system, in which the interaction between Cy3 and the substrate is reduced by its construction. The result is immediately visible in the microarrays; see figure 9, which displays clear intensity differences. Signal intensities of the (denatured and non-denatured) oligonucleotides are higher by a factor of about 5 when the linker is attached to the molecule, as demonstrated in figure 10.

5. Discussion and outlook

In this paper we have discussed the morphologies of unspecifically bound DNA deposited from a liquid drop. Depending on the solvent, substrate and droplet removal conditions a rich

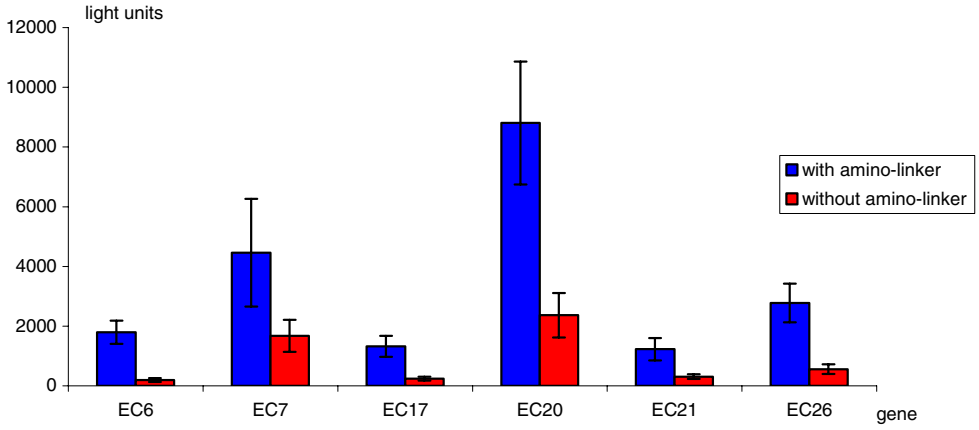

Figure 8. The amount of DNA immobilized on the microarrays in per cent. Scanner: arrayWoRx, (Cy3 (548/595); 0.1 s). The effect of the gene length is clearly visible (EC6: 6 bp long fragment etc).

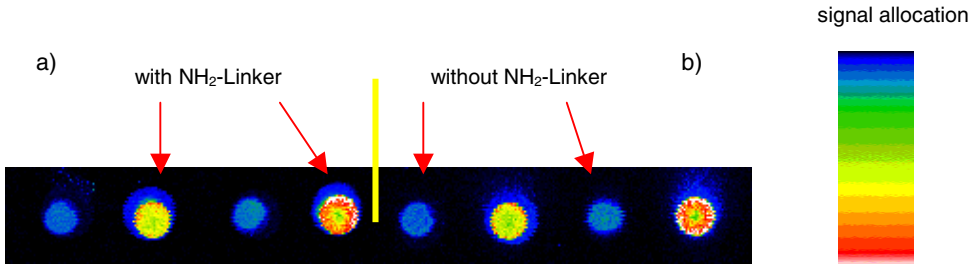

Figure 9. Views of a streptavidin-Cy3-labelled microarray; (a) without denaturation before labelling; (b) with the microarray denatured before labelling. (Scanner: scan array 3000; 90% laser power, 75% PMT sensitivity.)

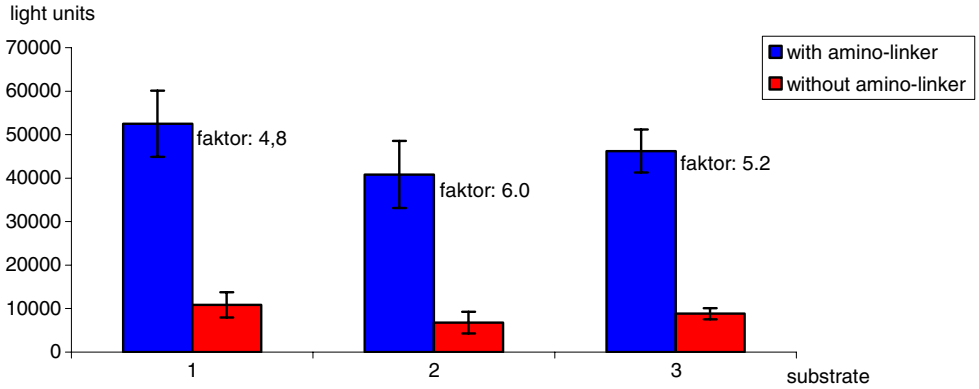

Figure 10. A graphical representation of the signal intensities obtained after immuno-labelling with streptavidin-Cy3. Substrate 1 was not denatured before labelling, while substrates 2 and 3 were denatured before labelling. (Scanner: scan array 3000; 90% laser power, 66% PMT sensitivity.)

variety of DNA morphologies were found. It is certainly safe to argue that both the variation of equilibrium aspects, such as solvent and surface conditions, and the complex dynamics of

the liquid drop contribute to this variety. The deposition of DNA by a droplet-based method must thus be considered as rather non-robust, as it depends on many details. Only under rather well-controlled conditions can this method thus lead to reproducible and controlled deposition patterns. In microarrays, reproducibility is controlled by empirically optimized protocols. For these systems, we have seen that the amount of unspecifically bound DNA can be experimentally quantified and controlled.

Nevertheless, one can also perceive that for future analysis, better-defined systems will be needed in order to reduce the large burden of complex data analysis needed to quantify expression data from today's high throughput devices. We believe that a better understanding of the mechanisms underlying both denaturation and hybridization of DNA at solid surfaces will be helpful for that purpose. For similar arguments in this direction, see also [28]. We believe that our results, in addition to their intrinsic interest, will be of relevance also for studies of further properties of DNA, e.g. its conduction properties [31], and phase transitions of DNA at the surface [45].

Acknowledgment

RB's work in the priority programme *Wetting and Structure Formation at Surfaces* was supported by the DFG under grant Bl-356/2-1.

References

[1] Blossey R 1995 *Int. J. Mod. Phys.* B **9** 3489
[2] Bonn D, Bertrand E, Meunier J and Blossey R 2000 *Phys. Rev. Lett.* **84** 4661
[3] Becker J, Grün G, Seemann R, Mantz H, Jacobs K, Mecke K R and Blossey R 2003 *Nat. Mater.* **2** 59
[4] Neto C, Jacobs K, Seemann R, Blossey R, Becker J and Grün G 2003 *J. Phys.: Condens. Matter* **15** 3355
[5] Neto C, Jacobs K, Seemann R, Blossey R, Becker J and Grün G 2003 *J. Phys.: Condens. Matter* **15** S421
[6] Montevecchi E and Blossey R 2000 *Phys. Rev. Lett.* **85** 4743
[7] Blossey R 2001 *Quantized Vortex Dynamics* (Berlin: Springer) p 421
[8] Blossey R 2001 *Ann. Phys., Lpz.* **10** 733
[9] Schäffer E, Harkema S, Blossey R and Steiner U 2002 *Europhys. Lett.* **60** 255
[10] Schäffer E, Harkema S, Roerdink M, Blossey R and Steiner U 2003 *Macromolecules* **36** 1645
[11] Schäffer, Harkema S, Roerdink M, Blossey R and Steiner U 2003 *Adv. Mater.* **15** 514
[12] Bonn D, Meunier J, Rolley E, Bausch R and Blossey R 2001 *Phys. Rev. Lett.* **87** 27601
[13] Blossey R 2002 *J. Low Temp. Phys.* **126** 355
[14] Bonn D, Kellay H and Meunier J 1994 *Phys. Rev. Lett.* **73** 3560
[15] Bausch R and Blossey R 1994 *Phys. Rev.* E **50** R1759
[16] Lorke A, Blossey R, Garcia J M, Bichler M and Abstreiter G 2002 *Mater. Sci. Eng.* B **88** 225
[17] Blossey R and Lorke A 2002 *Phys. Rev.* E **65** 021063
[18] Deegan R D, Bakajin O, Dupont T F, Huber G, Nagel S R and Witten T 1997 *Nature* **389** 827
[19] Deegan R D 2000 *Phys. Rev.* E **61** 475
[20] Deegan R D, Bakajin O, Dupont T F, Huber G, Nagel S R and Witten T 2000 *Phys. Rev.* E **62** 756
[21] Blossey R and Bosio A 2002 *Langmuir* **18** 2952
[22] Latterini L, Blossey R, Hofkens J, Vanoppen P, de Schryver F, Rowan A E and Nolte R J M 1999 *Langmuir* **15** 3582
[23] Bensimon A, Simon A, Chiffaudel A, Croquette V, Heslot F and Bensimon D 1994 *Science* **265** 2096
[24] Bensimon D, Simon A J, Croquette V and Bensimon A 1995 *Phys. Rev. Lett.* **74** 123
[25] Allemand J F, Bensimon D, Jullien L, Bensimon A and Croquette V 1997 *Biophys. J.* **73** 2064
[26] Abramchuk S S, Khoklov A R, Iwataki T, Oana H and Yoshikawa K 2001 *Europhys. Lett.* **55** 294
[27] Fisher B J 2002 *Langmuir* **18** 60
[28] Zhang L, Miles M F and Aldape K D 2003 *Nat. Biotechnol.* **21** 818
[29] Matsumoto S, Morikawa K and Yangida M 1981 *J. Mol. Biol.* **152** 501
[30] Ulman A 1991 *An Introduction to Ultrathin Organic Films* (New York: Academic)
[31] Heim T 2002 *Thése de doctorat* Université Lille 1 (unpublished)

[32] Fried M G and Bloomfield V A 1984 *Biopolymers* **23** 2141
[33] Bloomfield V A 1997 *Biopolymers* **44** 269
[34] Kleinschmidt A K and Zahn R K 1959 *Naturforschung* B **14** 770
[35] Mayor H D and Jordan L E 1968 *Science* **161** 1246
[36] Pietrzykowska I and Shugar D 1968 *Science* **161** 1246
[37] Vollenweider J, Sogo J M and Koller T 1975 *Proc. Natl Acad. Sci.* **72** 83
[38] Guttman S B 1992 *J. Struct. Biol.* **108** 162
[39] Rivetti C, Guthold M and Bustamante C 1996 *J. Mol. Biol.* **264** 919
[40] Crut A, Lasne D, Allemand J F, Dahan M and Desbiolles P 2003 *Phys. Rev.* E **67** 051910
[41] Kang S H, Shortreed M R and Yeung E S 2001 *Anal. Chem.* **73** 1091
[42] Nony L, Boisgard R and Aimé J P 2001 *Biomacromolecules* **2** 827
[43] Matulis D, Rouzina I and Bloomfield V A 2002 *J. Am. Chem. Soc.* **124** 7331
[44] Preuss S 2002 *Diplomarbeit* FH Aachen (unpublished)
[45] Heim T and Blossey R 2004 unpublished